Clin Exp Metastasis (2012) 29:927–938
DOI 10.1007/s10585-012-9481-5

RESEARCH PAPER

# Location matters: osteoblast and osteoclast distribution is modified by the presence and proximity to breast cancer cells in vivo

**H. K. Brown · P. D. Ottewell · C. A. Evans · I. Holen**

Received: 13 December 2011 / Accepted: 11 April 2012 / Published online: 6 May 2012
© Springer Science+Business Media B.V. 2012

**Abstract** Bone metastasis is a common incurable complication of breast cancer affecting around 70% of patients with advanced disease. In order to improve outcomes for these patients, the cellular and molecular mechanisms underlying bone metastasis need to be established. The majority of studies to date have focused on end-stage disease and little is known about the events taking place following initial tumour cell colonisation of bone. Here we report the results of a longitudinal study that provides detailed analysis of the spatial and temporal relationship between bone and cancer cells during progression of bone metastasis. Tumour growth in bone was initiated by intracardiac inoculation of MDA-MB-231-GFP breast cancer cells in immunocompromised mice. Differentiating between areas of bone in direct contact with the tumour and areas distal to the cancer cells but within the tumour bearing bone, we performed comprehensive analyses of the number and distribution of osteoclasts and osteoblasts. Tumour colonies were detectable in bone from day 10, while reduced trabecular bone volume was apparent from day 19 onwards. Cancer-induced changes in osteoblast and osteoclast numbers differed substantially depending on whether or not the cells were in direct contact with the tumour. Compared to naïve controls, areas of bone in direct contact with the tumour had significantly reduced osteoblast but increased osteoclast numbers, whereas the reverse was found in distal areas. Our data demonstrate that tumour cells induce substantial changes in the bone microenvironment prior to the appearance of bone lesions, suggesting that early therapeutic intervention may be required to oppose the tumour-induced changes to the microenvironment und thus tumour progression.

**Keywords** Breast cancer · Bone metastasis · Osteoblast · Osteoclast · Osteolysis · Bone microenvironment

**Abbreviations**

| | |
|---|---|
| Oc | Osteoclast |
| Ob | Osteoblast |
| PINP | Procollagen type I N-terminal propeptide |
| uCT | Microcomputed tomography |
| ELISA | Enzyme-linked immunoassay |
| H&E | Hematoxylin and eosin |
| TRAP | Tartrate-resistant acid phosphatase |
| GFP | Green fluorescent protein |
| NBP | Nitrogen-containing bisphosphonate |

## Introduction

Bone metastasis is a frequent feature of late stage breast cancer and currently patients mainly receive palliative treatment, as the disease is considered incurable. In breast cancer, bone metastases are associated with predominantly lytic bone lesions caused by tumour cells disrupting the fine-tuned balance between bone resorption (mediated by osteoclasts) and bone formation (mediated by osteoblasts) that exists during normal bone turnover [1]. The resulting osteolytic lesions are the main cause of morbidity and mortality and are a major clinical feature in this group of

**Electronic supplementary material** The online version of this article (doi:10.1007/s10585-012-9481-5) contains supplementary material, which is available to authorized users.

H. K. Brown (✉) · P. D. Ottewell · C. A. Evans · I. Holen
Academic Unit of Clinical Oncology, DU10, Medical School, University of Sheffield, Beech Hill Road, Sheffield S10 2RX, UK
e-mail: mdp08hkb@sheffield.ac.uk

patients. Understanding the underlying cellular and molecular mechanisms throughout tumour development in bone is key to the development of new and improved treatment strategies. To date, most studies have focused on end stage disease, with only little information on how and when small but established breast cancer colonies induce changes in bone cell number and distribution ultimately leading to overt bone destruction.

It is currently not possible to predict which patients will relapse after their initial treatment and subsequently develop bone metastases. Due to the lack of biological markers that can be applied in routine diagnosis, bone metastases are detected once the tumour is established and has formed radiologically detectable osteolytic bone lesions. Although there are effective therapies available to treat the resulting cancer-induced bone disease, it is currently not possible to prevent the development of bone metastases. The standard approved therapy for tumour-induced osteolytic bone disease is zoledronic acid, a member of the nitrogen-containing bisphosphonate (NBP) group [2]. The drug acts by reducing osteoclast activity via inhibition of the mevalonate pathway, thus counteracting the osteolytic effects induced by the tumour [3–6]. In addition, NBPs have been shown to exhibit direct and/or indirect anti-cancer effects in both in vitro [7] and in in vivo studies [8–10]. Despite the strong bone-sparing effects demonstrated in several in vivo studies, use of NBPs alone are not sufficient to eradicate tumour growth in models of multiple myeloma [11], breast cancer [12, 13] or prostate cancer [14]. In order to develop successful therapeutic strategies for prevention of bone metastasis, a better understanding of the early stages of bone metastasis is required. In particular, the initiating stages of the interaction between cancer cells and bone cells prior to the reduction of trabecular bone and the formation of osteolytic lesions are of interest. Analysis of these events is largely limited to the study reported by Phadke et al. [15], showing that the presence of cancer cells in bone results in reduced overall numbers of both osteoblasts and osteoclasts 4 weeks following intracardiac tumour cell implantation, but not at earlier time points. To our knowledge, no comprehensive histological analysis has been carried out charting changes in osteoblast and osteoclast numbers associated with breast tumour progression in bone. Here we present a detailed study of the spatial and temporal changes of both tumour cells and bone cells, including time points prior to the appearance of osteolytic bone disease. The development of human breast cancer growth and the resulting cancer-induced bone disease from early, intermediate to late stage disease was characterised and changes in bone cell numbers were determined in detail. Our data demonstrate that in the stages prior to detectable cancer-induced trabecular bone loss the presence of small tumour colonies can profoundly modify the bone microenvironment, and that the nature of these changes depends on whether there is direct contact between tumour cells and bone cells. This new information on early interactions between tumour cells and the bone microenvironment may have implications for optimisation of treatment of bone metastasis, in particular when to initiate therapy.

## Materials and methods

### Maintenance of cell line and tumour growth model

Human MDA-MB-231 breast cancer cells stably expressing green fluorescent protein (GFP) were maintained in RPMI-1640 (GIBCO) supplemented with 10% fetal calf serum and 1% penicillin/streptomycin (PAA Laboratories). Cells were grown at 37°C and 5% $CO_2$.

MDA-MB-231-GFP cells ($1 \times 10^5$) were injected directly into the left heart ventricle of 6-week-old female balb/c nu/nu mice under general anesthesia induced by 100 mg/kg ketamine (Fort Dodge Animal Health Ltd) and 15 mg/kg xylazine (Bayer plc). All experiments were carried out in accordance with local guidelines and with Home Office approval under project license 40/2972 held by Professor N.J. Brown, University of Sheffield, United Kingdom. Two independent in vivo experiments, and a total of 85 animals were used for the entire study (25 naïve and 60 tumour-bearing animals used in total). Animals were randomly grouped into each of the five sequential time points ($n = 12 + 5$ naïve/time point) covering early (day 10 and 15), intermediate (day 19 and 24) and late stage disease (end of protocol (EOP) including days 28–33, Fig. 1a). Only animals with detectable bone tumours were entered into subsequent analysis and confirmation of osseous tumour growth was carried out by GFP imaging (Lighttools). On day of sacrifice, hind legs were fixed in 4% PFA for 72 h and scanned by μCT. Subsequently, the bones were decalcified in 0.5 M EDTA and 0.5% PFA for 2 weeks before embedding in paraffin wax.

### Measurement of tumour area on histological sections

Histologic sections (3 μm) of decalcified hind legs were stained with H&E and analysis was carried out using a Leica BMRB upright microscope with a 4× objective and Osteomeasure software (Osteometrics, Inc.). Tumour area (expressed as % intraosseous tumour area) was measured by drawing around the inner surface of the bone marrow cavity in the metaphysis as well as the tumour area in this region. 2–3 non-serial histologic sections per sample were scored.

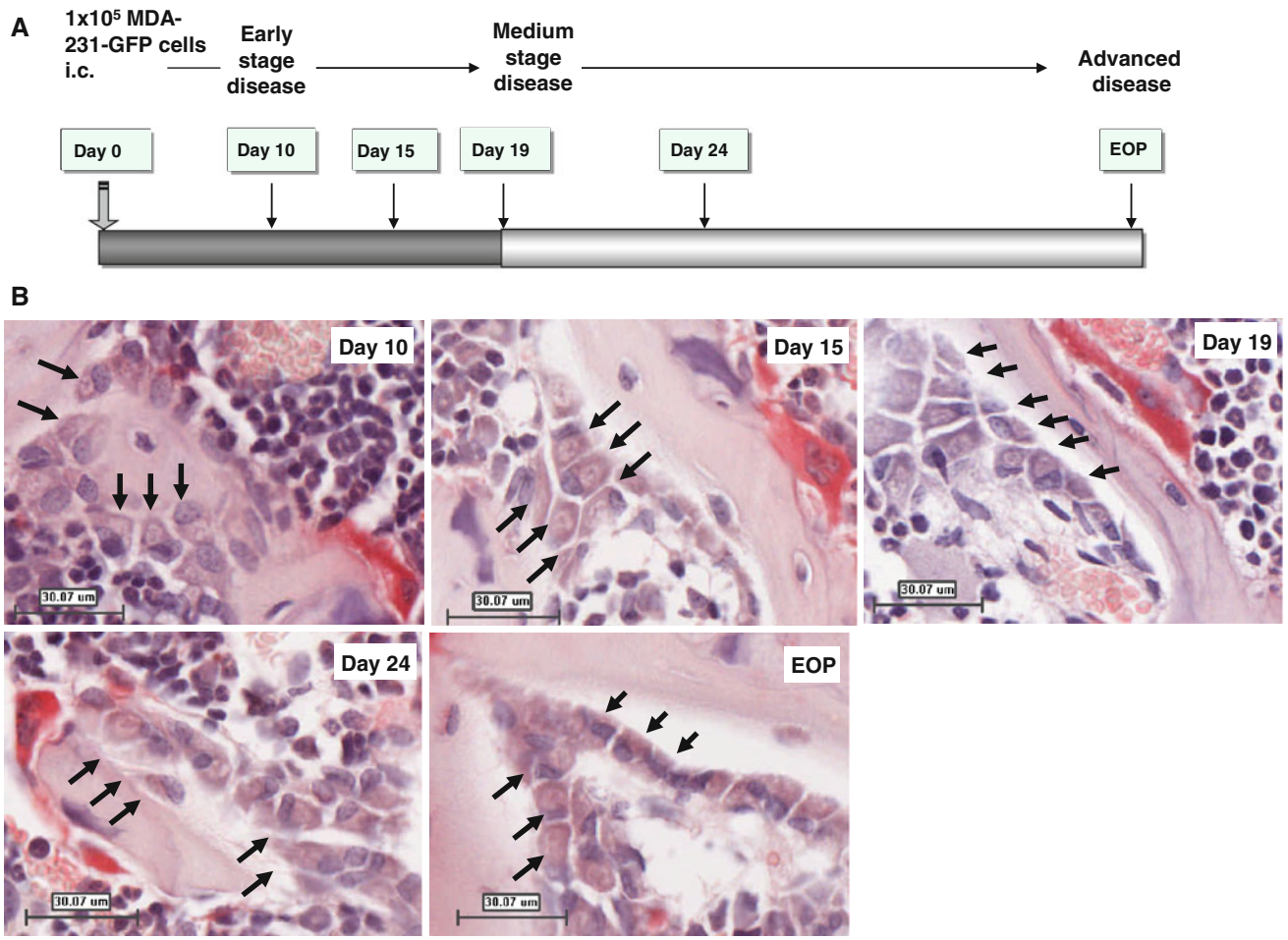


**Fig. 1** Study outline and examples of osteoblasts. **a** Experimental protocol. Following intracardiac inoculation of $1 \times 10^5$ MDA-MB-231-GFP tumour cells on day 0, animals were divided into five groups to cover different stages of tumour progression at day 10, 15, 19, 24 and EOP (depending on morbidity, day 28–33). 12 tumour-bearing and five naive animals were sacrificed per time point. **b** Examples of TRAP stained histological sections showing osteoblast morphology at 10, 15, 19, 24 and 33 days post initiation of the experiment. *Arrows* indicate osteoblasts aligned along trabecular bone surfaces. *Scale bar* = 30.07 μm

## Immunohistochemistry

Immunohistochemistry for the cell proliferation antigen Ki67 was carried out as previously described [16] using a mouse monoclonal antibody specific for human Ki67 (Clone MIB-1, DakoCytomation; 1:125 dilution) followed by a biotin-conjugated anti-mouse secondary antibody (Vector laboratories; 1:200). Two non-serial sections per tumour sample were stained and the number of Ki67-positive cells per tumour area ($mm^2$) were scored using a Leica BMRB upright microscope with a 10× objective and OsteoMeasure software (Osteometrics). Staining for human RANKL was performed using a polyclonal goat anti-human RANKL antibody (AF626, R&D systems; 1:50 dilution) followed by a biotinylated anti-goat secondary antibody (Vector laboratories; 1:200 dilution).

## TRAP and Goldner trichrome staining

Tartate-resistant acid phosphatase (TRAP) staining was used for all osteoclast (Oc) and osteoblast (Ob) quantifications. Briefly, dewaxed sections were incubated in acetate-tartrate buffer at 37°C for 5 min followed by incubation in naphthol AS-BI phosphate, dimethylformamide in acetate-tartrate buffer for 30 min at 37°C. Finally sections were placed in a solution containing sodium nitrite, pararosaniline and acetate-tartrate buffer for 15 min at 37°C, before counterstaining in haematoxylin. The number of TRAP stained osteoclasts per millimeter trabecular bone surface was scored using a Leica RMRB upright microscope with a 10× objective and OsteoMeasure software (Osteometrics). In the same sections, osteoblasts were scored per millimeter trabecular bone surface in line with previously published studies [17–20]. For

clarification, example images of osteoblasts at each time point are shown in Fig. 1b. Analysis was performed using the following criteria: (a) total number of Oc and Ob on the entire trabecular bone surface, (b) the number of Oc and Ob per mm trabecular bone surface where the bone cells were in direct contact with tumour tissue (Category 1, Fig. 5a) and (c) the number of Oc and Ob per mm trabecular bone that were not in direct contact with tumour cells (Category 2, Fig. 5a). Osteoclast size was determined by measuring osteoclast area in the same sections and data are expressed as mean osteoclast size ($mm^2$). At least two non-serial sections were analysed per sample. In naïve mice the Oc and Ob number of the entire trabecular none surface was assessed.

The Masson-Goldner trichrome staining (Merck) was performed to the manufacturers instructions and the stained sections were used for exemplary visualisation purposes only.

### Microcomputed tomography imaging

Microcomputed tomography analysis was carried out using a Skyscan 1172 X-ray-computed microtomograph (Skyscan). Imaging was carried out at a voltage of 50 kV and a current of 200 μA with a medium camera resolution of 2000 × 102, an aluminium filter of 0.5 mm and pixel size was set to a dimension of 4.3 μm. Scanning was initiated from the proximal tibia or distal femur. For each sample, images were reconstructed with NRecon software. The volume of interest (VOI) was then specified by interactively drawing on the two-dimensional acquisition images. For trabecular bone measurements, the VOI was composed only of cancellous bone, and the cortices were excluded. Trabecular bone volume (BV/TV in %, which is defined as the percentage of the volume of interest occupied by binarised solid objects) was calculated covering 1 mm, starting from the lowest part of the growth plate.

### Statistical analysis

Prism Graphpad (Version 5.0a) was used for all statistical analysis. Analysis was by Mann–Whitney or Kruskall–Wallis with Dunns post test. The applied test is indicated in each figure legend. Data is presented as mean ± SEM and we have interpreted differences as being significant at $p \leq 0.05$.

## Results

We performed a comprehensive study of breast tumour growth in bone investigating tumour cell-bone cell interactions from early (day 10–15 following tumour cell injection) to intermediate (day 19 and 24) and end-stage disease (day 28–33, EOP). All time points ($n = 12$ mice per time point) included five naïve mice in order to compare tumour bearing to non-tumour bearing bone. A range of techniques was used to assess bone integrity, tumour area and bone-tumour cell interactions at each time point. In addition to characterising the effects of tumour progression on osteoclasts, we focused on the analysis of osteoblasts due to the lack of information regarding their role in breast cancer-induced bone disease from in vivo studies.

### Characterisation of osseous MDA-MB-231 tumour development

Hind legs with confirmed osseous tumour growth (shown by GFP imaging, Fig. 2a) were used for subsequent histological analysis. Tumour area in the metaphysis was analysed on histological sections of tibias and femurs. In specimens taken on day 10 to EOP the percentage of the bone marrow cavity occupied by tumour increased steadily with time from tumour cell injection (Fig. 2b). Examples of tumour foci in bone are depicted on images of Goldner trichrome stained sections (Fig. 2d).

In order to investigate tumour viability at each time point we performed Ki67 immunohistochemistry, which allows the quantification of actively proliferating human breast cancer cells (Fig. 2c, e). The number of Ki67 positive cells remained near constant throughout the different stages of tumour progression. It was not possible to perform comprehensive Ki67 analysis on the day 10 tumours due to the limited tumour material available at this early time point.

### Development of osteolytic lesions

While it is well known that breast cancer metastases to bone are the cause of osteolytic bone disease, it may be important to identify the exact stage at which cancer cells initiate bone destruction in order to successfully treat and ultimately prevent it. When analysing μCT cross sections of hind legs, overt osteolytic lesions were apparent in 100% of tumour bearing mice from day 19 onwards (Fig. 3a). The presence of osteolytic lesions is currently used as a clinical indication for the presence of metastatic bone disease. However, it is likely that the tumour cells lodge on trabecular bone surfaces and establish here before affecting the cortical bone area thus forming radiographically detectable lesions. In order to analyse the more detailed effect of longitudinal breast cancer growth on trabecular bone destruction, μCT analysis of trabecular bone in the distal femur and proximal tibia was performed. MDA-MB-231-GFP tumour cell growth reduced trabecular bone

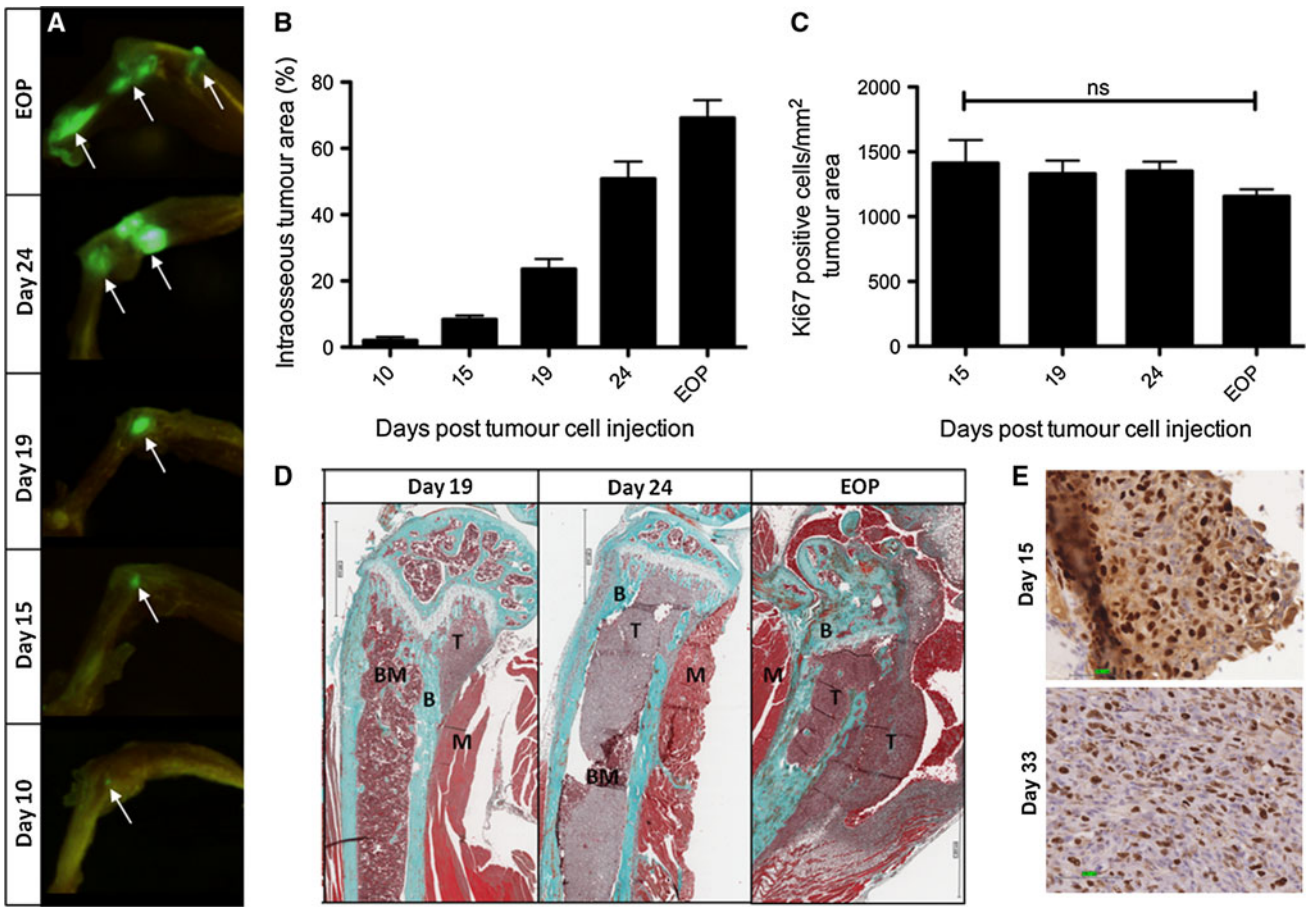


**Fig. 2** Characterisation of longitudinal breast tumour growth in bone. **a** In vivo GFP imaging of hind legs was used to confirm tumour growth. *Arrows* indicate tumour foci. **b** Histological analysis (H&E stained sections) of tumour area in hind legs (presented as % intraosseous tumour area). Number of mice included in analysis: day 10 $n = 4$, day 15 $n = 7$, day 19 $n = 8$, day 24 $n = 9$, EOP $n = 6$. A minimum of two sections per sample was analysed. **c** Ki67 staining was performed to assess tumour cell proliferation. Kruskal–Wallis and Dunn's post test. **d** Visualisation of tumour growth for each time point by Goldner's trichrome stain (4× objective). *T* tumour, *BM* bone marrow, *B* bone, *M* muscle, *scale bar*: 1 mm. **e** Example images of small tumour colonies (day 15) and end stage disease (EOP) stained for Ki67 (*scale bar*: 100 µm, 20× objective)

volume (% BV/TV) from day 19 onwards compared to the bone volume in naïve mice with a significant reduction on day 24 (5.51 vs. 11.67, $p < 0.001$) and at EOP (3.41 vs. 12.1, $p < 0.001$, Fig. 3b). The µCT data indicate that smaller tumour colonies (day 10 and 15) do not induce a detectable reduction in trabecular bone volume when compared to naïve bones. Further µCT analysis suggested that decreased trabecular number appeared to be mainly responsible for the reduction in % BV/TV in tumour bearing mice from day 19 to EOP (Fig. 3c).

## Bone cell distribution changes with increasing tumour burden

After having established the time frame in which tumour cells induce a detectable reduction in trabecular bone volume we next carried out comprehensive analysis of the effects of small, intermediate and large tumour colonies on two bone cell types, bone resorbing osteoclasts (Oc) and bone forming osteoblasts (Ob). We first assessed the differences between total Oc and Ob numbers in tumour bearing compared to naïve (non-tumour bearing) mice.

In agreement with other studies, we found a significant increase in the total number of osteoclasts in trabecular bone from breast cancer bearing compared to naïve mice. The number of resorbing cells increased from day 19 onwards, in line with the detected onset of trabecular bone volume reduction (µCT). Osteoclast numbers were significantly higher than in naïve controls on day 19 (5.8 vs. 4.98, $p < 0.05$) and on day 24 (6.02 vs. 4.48, $p < 0.01$, Fig. 4a).

When analysing the effects of the tumour on osteoblasts, the most profound changes were shown to be taking place before trabecular bone destruction was apparent, with a significant increase in osteoblast numbers per mm bone

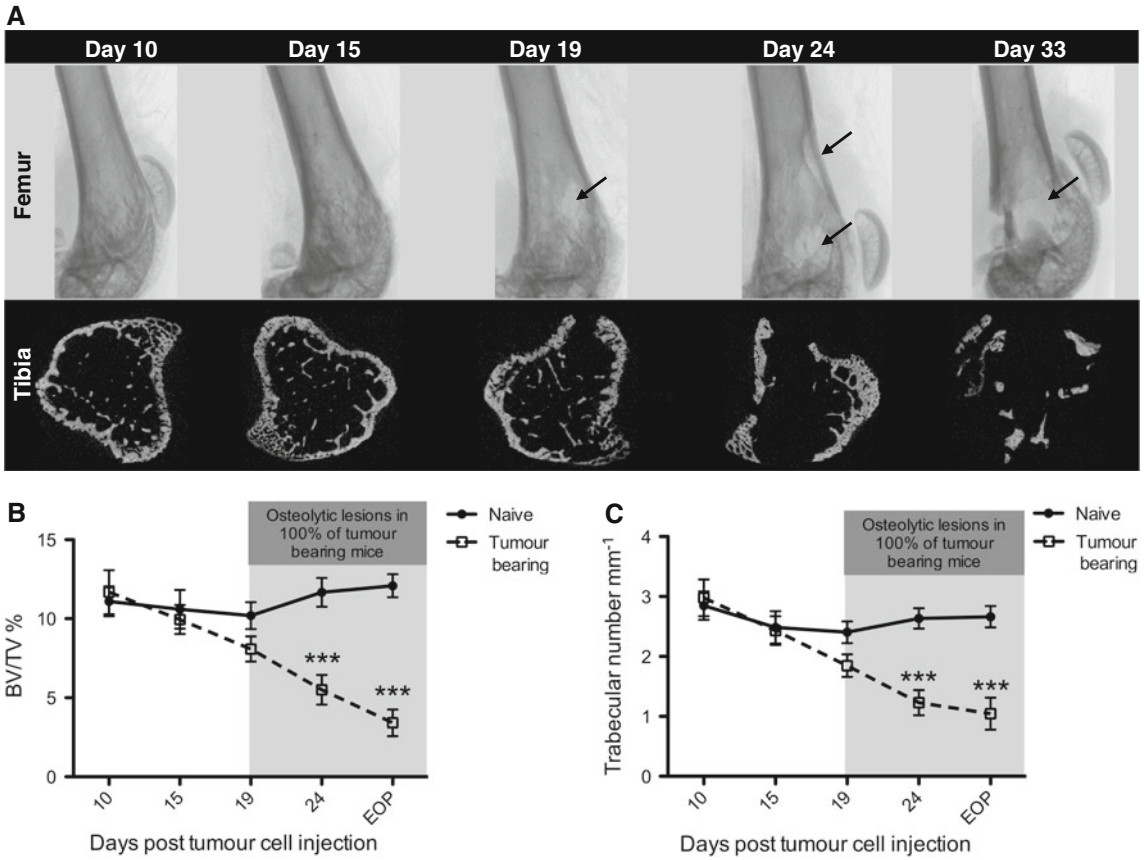


**Fig. 3** Development of osteolytic lesions. **a** *Top panel*: example radiographs of the distal femur for each time point taken from μCT analysis. *Arrows* indicate osteolytic lesions. *Bottom panel*: visualisation of trabecular bone on uCT cross-sections of the proximal tibia. **b** μCT analysis of trabecular bone is depicted as % BV/TV and was carried out for the proximal tibia and distal femur of tumour bearing bones. Day 10 $n = 6$ mice, day 15 $n = 10$, day 19 $n = 8$, day 24 $n = 11$, EOP $n = 6$ mice, naïve $n = 5$/time point. **c** Analysis of trabecular number for proximal tibia and distal femur. Mann–Whitney test was carried out for each time point separately, *** is $p < 0.001$ compared to naïve mice

surface compared to non-tumour bearing mice on day 15 (13.48 vs. 7.39, $p < 0.001$, Fig. 4b). In contrast to osteoclasts, osteoblast numbers of tumour-bearing mice were dramatically reduced with the onset of detectable bone disease, dropping below the levels found in naïve animals at EOP (2.19 vs. 6.75, $p < 0.001$). At early stages of disease (10 days post tumour inoculation) there was no significant difference in osteoclast or osteoblast numbers between naïve and tumour bearing animals.

Analysis of the ratio between osteoblasts and osteoclasts in non-tumour bearing mice showed that this was maintained at a constant level (ranging from 1.38 to 1.61) throughout the duration of the experiment. In early stages the Ob/Oc ratio of tumour bearing animals was higher compared to naïve mice with a significant increase on day 15 (2.96 vs. 1.38, $p < 0.001$, Fig. 4c). As expected, corresponding with the onset of osteolytic bone disease the Ob/Oc ratio dropped at the end of the protocol below that of naïve mice (0.51 vs. 1.47, $p < 0.01$), mainly driven by a substantial reduction in osteoblast numbers.

## Tumours do not affect bones through systemic effects

The animal model used in this study leads to tumour growth predominantly in the hind legs but, especially in early disease, the tumour foci are not always present in both femurs and both tibias. We therefore investigated if local tumour colonies in bone have an effect on bone structure in adjacent, tumour-free bones. μCT analysis showed no statistically significant change in trabecular bone volume in non-tumour bearing bones compared to naïve mice at any time point (supplementary figure 1A).

We also assessed whether the changes in total osteoclast and osteoblast numbers were induced by systemic factors, or were limited to the tumour bearing leg. To investigate systemic markers, sera collected from fasted animals were used for analysis of the bone formation marker PINP and the bone resorption marker CTX. In both cases no significant change could be detected when comparing levels from tumour-bearing mice to naive, age-matched animals (supplementary figure 1B and C). In addition, serum

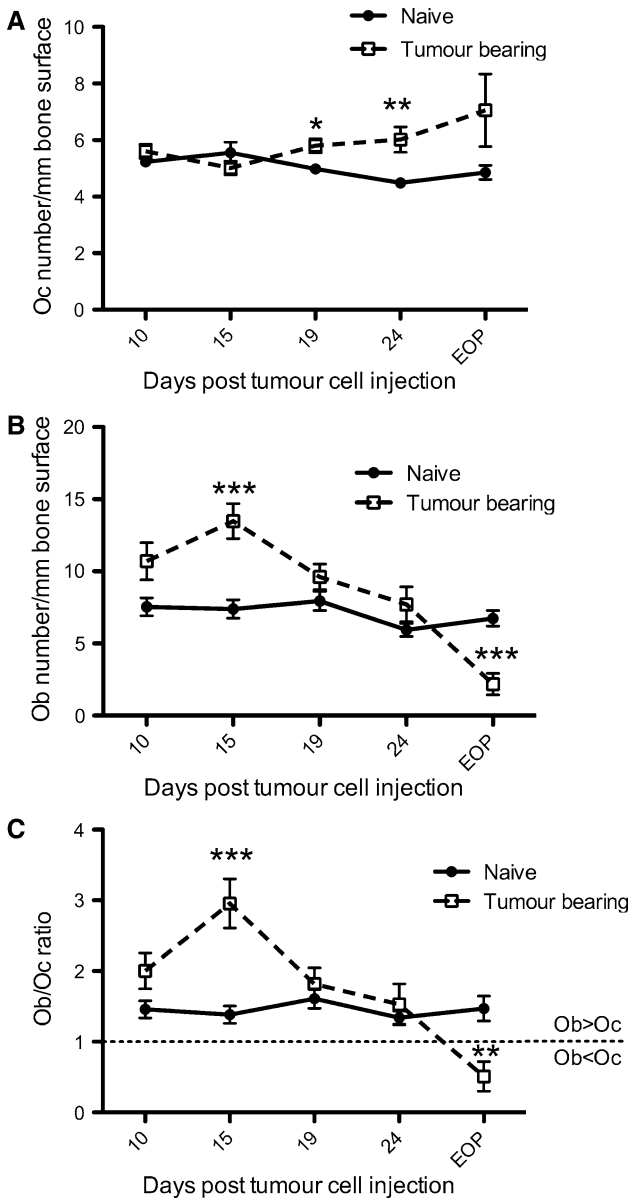


**Fig. 4** Effects of increased tumour burden on bone cell distribution Total osteoclast (**a**) and osteoblast (**b**) numbers per mm trabecular bone surface in the proximal tibia and distal femur were assessed on TRAP stained histological bone sections. **c** Osteoblast/osteoclast ratio of total bone cell numbers. The following number of mice were used for TRAP analysis: day 10 $n = 5$, day 15 $n = 6$, day 19 $n = 8$, day 24 $n = 9$, EOP $n = 6$, naïve $n = 5$/time point. Mann–Whitney test was performed for each time point separately, $*p < 0.05$, $**p < 0.01$, $***p < 0.001$ compared to naïve mice

measurements of the osteoclast-inducing molecule RANKL (murine) as well as the expression of the Wnt-pathway inhibitor sclerostin (human) were performed. There was no significant increase in serum levels of RANKL and sclerostin in tumour-bearing compared to naïve animals (supplementary figure 1D and E). However, sections stained by immunohistochemistry showed strong expression of RANKL by the tumour (Fig. 6d), suggesting direct effects of the tumour cells on the osteoclasts. These results, combined with the unchanged bone marker levels and the lack of effects on bone integrity, confirm the absence of systemic effects of the tumour on bone.

Taken together, our results show that small to medium sized breast tumour foci in bone have substantial effects on bone cells within the affected bone. Total osteoblast numbers change before the entire osteoclast population on trabecular bone increases and osteolytic bone disease is detectable by μCT.

## Osteoblast and osteoclast numbers change according to their proximity to the tumour

As previous analysis indicated a localised effect of the tumour on bone destruction; we further investigated whether or not the changes in osteoblast and osteoclast numbers were dependent on direct cancer cell-bone cell contact. To do this, two categories of bone cells in tumour bearing bones were scored: Category (1) osteoclasts or osteoblasts in direct contact with tumour cells, and category 2) osteoclasts or osteoblasts not in direct contact with the tumour (Fig. 5a). Quantification of osteoclast numbers in these two categories revealed a clear differential effect of the tumour depending on the proximity of the bone resorbing cells to the cancer cells. Osteoclast numbers in direct contact with tumour cells (category 1) where significantly increased compared to those osteoclasts away from the tumour colony (category 2). In fact, these cells away from the tumour remained at a level similar to naïve animals throughout the whole experiment. This differential effect was detected at all time points, with significantly different osteoclast numbers/mm bone surface on day 10, 15, 19, 24 and at EOP (day 10: 18.7 vs. 5.26, $p < 0.001$; day 15: 13.67 vs. 4.12, $p < 0.001$, day 19: 11.41 vs. 3.87, $p < 0.001$; day 24: 11.7 vs. 2.92, $p < 0.001$ and EOP: 9.79 vs. 3.15, $p < 0.01$, Fig. 5b). The discrepancy between the increased overall osteoclast number at later stages of tumour growth compared to naïve mice (day 19, 24 and EOP, Fig. 4a) and the decrease in osteoclasts in contact with the tumour in the differential analysis (day 24 and EOP, Fig. 5b) is likely due to the differences in bone surface available for scoring at these later time points.

Intriguingly, analysis showed that the presence of tumour colonies had the exact opposite effect on the two categories of bone forming osteoblasts than on bone resorbing osteoclasts. 15, 19 and 24 days post tumour cell injection the osteoblast population away from the tumour colony was significantly increased compared to those in direct contact with the tumour ($p < 0.001$ with 16.04 vs. 3.44 on day 15, $p < 0.001$ with 13.15 vs. 2.84 on day 19, $p < 0.001$ with 14.62 vs. 1.06 on day 24 and $p < 0.05$ with

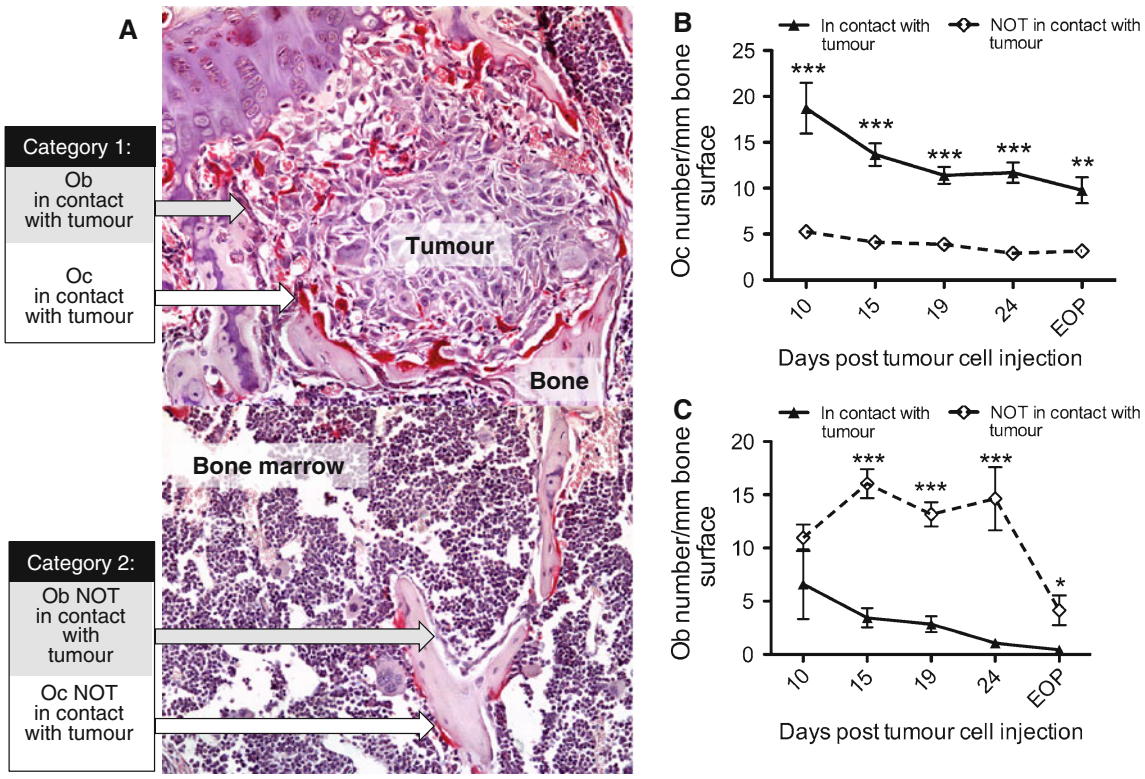


**Fig. 5** The proximity to tumour cells determines changes in osteoblast and osteoclast numbers. **a** Example TRAP section showing the two location dependent categories used for scoring of osteoclasts (Oc) and osteoblasts (Ob): category (1) Oc and Ob in direct contact with cancer cells and category (2) Oc and Ob not in direct contact with cancer cells but in the same tumour bearing femur/tibia. Analysis was carried out on at least two non-serial TRAP stained sections. **b** Quantitative results for osteoclast and **c** osteoblast numbers in tumour bearing mice. The following number of tumour bearing animals were included for each time point: day 10 $n = 5$, day 15 $n = 6$, day 19 $n = 8$, day 24 $n = 9$, EOP $n = 6$. Mann–Whitney test for each time point separately, $*p < 0.05$, $**p < 0.01$, $***p < 0.001$

4.14 vs. 0.43 at EOP, Fig. 5c). From day 10 onwards a reduction in osteoblast numbers of category (2) was found while osteoblasts in category (1) decreased from day 24 onwards.

The data show that the presence of breast cancer in bone has a differential effect on both osteoclasts and osteoblasts depending on their proximity to the tumour and that the development of cancer-induced bone disease involves changes to both cell types.

## Direct tumour cell contact increases osteoclast size

Because of the clear location-dependent effect of the tumour on bone cell numbers, morphological changes to osteoclasts were investigated. It has been proposed that cultures of large osteoclasts (>10 nuclei) are more likely to be actively resorbing than small osteoclasts (<5 nuclei) [21]. Since the quantification of nuclei on histological sections is difficult, the mean osteoclast area (measured in $mm^2$) of tumour-bearing mice was compared to naïve animals. Two time points were chosen for analysis, day 15 and 19, due to the first detectable changes in bone cell numbers on these days. Tumour-bearing animals had larger osteoclasts compared to naïve mice (day 15 $1.8 \times 10^{-4}mm^2$ vs. $1.4 \times 10^{-4}mm^2$, $p < 0.05$ and day 19 $2.1 \times 10^{-4}mm^2$ vs. $1.4 \times 10^{-4}mm^2$, $p < 0.001$, Fig. 6a). Further location-dependent analysis revealed that the increase in osteoclast size in tumour-bearing mice was due to large osteoclasts in direct contact with the tumour cells (Fig. 6b). Osteoclasts in contact with tumour had a mean size of $3.3 \times 10^{-4}mm^2$ compared to those distal to the tumour with $1.3 \times 10^{-4}mm^2$ on day 15 ($p < 0.001$) and $3.3 \times 10^{-4}mm^2$ compared to $1.5 \times 10^{-4}mm^2$ on day 19 ($p < 0.001$). The TRAP positive cells away from the tumour were shown to be of a similar size as in naïve animals. Furthermore, RANKL expression by the tumour cells was detected at all time points (Fig. 6d). The data strongly suggest that cell–cell contact is required for the tumour-induced changes in osteoclast size indicating a localised effect of the tumour on osteoclasts.

## Discussion

In this study we have characterised the cellular interactions associated with different stages of bone metastasis progression, investigating the temporal and spatial relationship

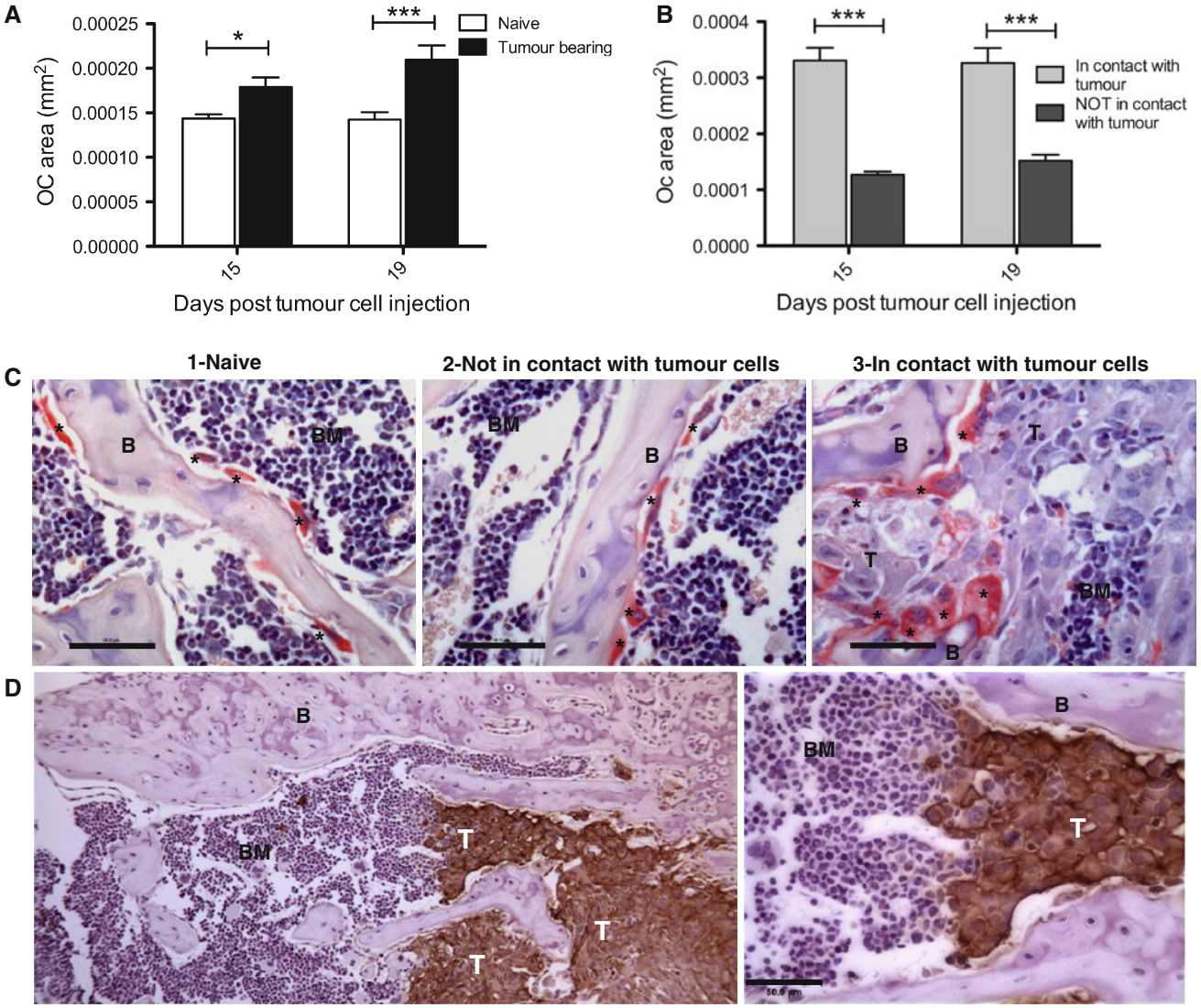


**Fig. 6** Osteoclast size (area in $mm^2$) was quantified on TRAP stained sections (20× objective). **a** Mean osteoclast area in naïve vs. tumour-bearing mice. **b** Mean osteoclast area in tumour-bearing animals differentiating between Ocs in direct contact with tumour cells and NOT in direct contact with the tumour. Mann–Whitney test for each time point separately, $*p < 0.05$, $***p < 0.001$. **c** Example images of TRAP sections for (1) naïve mice, (2) not in contact and (3) in contact with tumour (20× objective, *Oc (*red*). **d** Example images of human RANKL staining (brown, 10× and 40× objective). *B* bone, *BM* bone marrow, *T* tumour, *scale bar* = 50 µm. (Color figure online)

between breast cancer cells, osteoblasts and osteoclasts. Although tumour growth was clearly evident from day 10 onwards, tumour-induced decreases in trabecular bone volume did first become significant at day 24. These data show that there is a lag-phase between the initial growth of the tumour and the bone effects becoming detectable by µCT, and that studies of the latter require methods that capture cellular and molecular changes of the bone microenvironment. We therefore went on to investigate the effects of tumour growth on bone using bone histomorphometry, measurements of soluble bone markers and tumour/bone gene expression. These detailed analyses demonstrated that cancer-induced bone destruction is a localised process within the tumour-bearing bone, affecting trabeculae in direct contact or in close proximity (within the tumour-bearing bone) to the tumour colony. Our results are in agreement with those reported by Clohisy et al. [22], showing that breast cancer-induced bone disease is associated with focal lesions rather than induction of systemic bone disease. Assessment of total osteoclast numbers showed that this was only elevated from day 19 onwards, in accordance with the onset of reduced trabecular bone volume. Small tumour colonies had no significant effect on the total number of osteoclasts. Few previous studies have investigated the temporal progression of tumour-induced effects, but changes in osteoclast numbers have been described after intrafemoral injection of the osteosarcoma cell line 2472 into C3H/He mice [23]. In this primary bone

tumour model, osteoclast numbers increased from 6 to 9 days post tumour cell injection compared to sham injected bones. However, osteoclast numbers then dropped at day 12, despite significant osteolysis being detected from day 9 onwards. Both studies indicate that not only the total number of osteoclasts, but also their location and resorptive activity, determines the extent of the bone lesions.

In contrast to the perception that effects only on osteoclast are responsible for breast cancer-induced bone disease, our data showed that the presence of tumour colonies also had a significant effect on the total number of bone forming osteoblasts. Bone remodelling in healthy individuals is a highly controlled process with coupled cycles of bone resorption followed by bone formation [1]. Our data suggest that this balance is disrupted during the early stages of tumour growth, prior to detection of excessive bone resorption, and that this is reflected by biphasic changes in osteoblast numbers. This novel observation is in agreement with reports identifying the osteoblast as a crucial factor of breast tumour cell homing and progression in bone. Direct interactions between osteoblasts and MDA-MB-231 cells are demonstrated in a 3-dimensional osteogenic tissue model grown from the murine MC3T3-E1 pre-osteoblast cell line [24]. In this model, immature culture conditions were found to be more beneficial to cancer cell colonization, while mature osteoblast cultures were required for tumour expansion. Intratibial co-injection of the pre-osteoblastic MC3T3-E1 cell line and MDA-MB-231 cells have been shown to induce significantly higher tumour burden compared to athymic mice injected with the cancer cells alone, supporting a role for osteoblasts in tumour development [25]. One possible mechanism responsible for the increase in osteoblast numbers is that increased levels of osteoclast activity at the tumour-bone interphase results in a localised raise in extracellular calcium levels. It is well established that osteoblast maturation and proliferation is stimulated by extracellular calcium, as part of the tight coupling mechanism between bone formation and resorption [26]. In support of the direct effect of MDA-MB-231-GFP cells on the osteoclasts was the direct contact between the cells and the expression of RANKL by the tumour cells.

While most recent research has focused on the osteoblast-tumour cell interactions at the homing stage of metastatic disease [27], their role in the intermediate stages of tumour growth, like the escape from quiescence and the switch from microenvironment-dependent to -independent growth, are equally important. Our data add to the understanding of these processes by showing that osteoblasts, in addition to osteoclasts, may also be relevant during the transition of micro- to macro-metastatic growth. These findings are in agreement with one of the few studies investigating the cellular composition of bone biopsies from metastatic foci from breast cancer patients [28]. Analysis showed increased osteoclast and osteoblast numbers in biopsies with small to medium cancer colonies (bone marrow cavity covered to 7.5 or 24.4% by tumour) compared to non-tumour bearing control samples. Biopsies with larger tumours (tumour covering 47.1% of the bone marrow cavity) had decreased osteoblast and osteoclast numbers compared to tumour-free biopsies. The discrepancy in osteoclast numbers in comparison to the present data could be explained by differences between a mouse model and human biopsies and that total tumour burden in the biopsy cannot be assessed due to the relatively small area available for investigation.

Information on early stage breast cancer and the related changes to the bone microenvironment is largely limited to the report of Phadke et al. [15], who found a tumour progression-dependent reduction of osteoclast and osteoblast numbers 4 weeks after MDA-MB-435 tumour cell implantation. The group showed that the decrease in osteoblast number was associated with an increase in osteoblast apoptosis. In agreement with this, we also found an inhibitory effect of large tumour colonies on osteoblasts and osteoclasts using MDA-MB-231 cells. The increase in osteoblast numbers we found in early stages of progression were not identified in the model used by Phadke et al., and further studies are required to determine if this is due to the use of different breast cancer cell lines.

In order to identify the underlying molecular mechanisms involved in the alteration in total bone cell numbers, we next assessed whether the cellular changes were associated with any systemic effects on bone. The lack of bone loss assessed by μCT in non-tumour bearing legs strongly suggested the involvement of only local interactions, within the affected bone. In agreement with this, serum concentrations of both bone formation and resorption markers were unchanged in tumour-bearing animals compared to naïve. The localised tumour effects were further supported by the finding that increased osteoclast size was confined to the tumour-bone interphase in areas with bone cell-tumour cell contact. In studies of bone metastasis, the spatial relationship between different cell types is rarely taken into account, and it is unclear how far secreted molecules can diffuse in bone at a concentration high enough to induce cellular changes. Whereas in the majority of studies only the overall number of osteoclasts is investigated, our data suggest that it may be important to distinguish between the proximity of bone cells to tumour cells in studies of early metastatic events.

Surprisingly, tumour-induced changes in osteoblast numbers did not rely on direct cell contact, indicating the involvement of localized changes in soluble factors (like extracellular calcium) as well as surface molecules. However, it is not clear if these changes are downstream effects resulting from the local cancer-induced changes in bone

turnover. Molecular mechanisms that may be involved include the RANK/RANKL/OPG system, as well as the Wnt-pathway inhibitors DKK1 and sclerostin, molecules with an established role in regulation of bone turnover. Murine RANKL levels have been shown to be increased in serum of animals bearing intratibial prostate cancer colonies [29] compared to naïve control mice, and sclerostin was shown to be expressed by MDA-MB-231 cells in vitro [30] resulting in inhibition of osteoblast differentiation. In addition, osteoblasts have been reported to produce a specific range of bone-related cytokines after stimulation with MDA-MB-231 cells, including IL-6, IL-8 and MCP-1 [31]. In the in vivo setting, the effects of these factors may be limited to the bone microenvironment, as we did not detect changes in serum levels of RANKL and sclerostin in this study. The bone-specific nature of the changes is further supported by our own pilot data, showing increased levels of DKK1 and SFRP1 gene expression in MDA-MB-231 tumours isolated from bone, compared to from the same tumours implanted subcutaneously (supplementary table 1).

So what does this study tell us about the early stages of breast cancer bone metastasis and what are the clinical implications? Our data support that once tumour colonies reach a particular size, they induce a localized increase in osteoclast activity/number at the tumour–bone interface, causing an elevation of extracellular calcium levels accompanied by the well-established release of bone-associated tumour-growth factors. This, in turn, results in increased osteoblast differentiation to compensate for the elevated bone resorption, generating localized increases in osteoclast-stimulating RANKL on the surface of the osteoblasts. At this point, bone lesions appear and the latter stages of the disease are predominantly osteoclast-driven. These interactions suggest that the key steps to target in order to effectively treat bone metastasis is to either prevent tumour colonies from reaching a critical size, or to prevent bone resorption at earlier stages than in current clinical practice. Early administration of anti-resorptive agents like zoledronic acid and denosumab would be expected to inhibit the progression of bone metastasis. However, the picture is even more complex, as demonstrated by the recently published AZURE breast cancer trial that combined adjuvant chemotherapy with intensive inhibition of bone resorption [32]. Tumor progression in bone was only reduced in post-menopausal patients, indicating that additional endocrine factors also play an important part in bone metastasis. We have shown that detailed analyses reveal tumour-induced changes to the bone microenvironment, and suggest that this approach will be essential to establish effects of therapeutic interventions.

**Acknowledgments** Breast Cancer Campaign, UK, generously supported this study. We would also like to thank Mr Ken Mann for performing the RANKL immunohistochemistry and Dr Simon Cross for his help with the evaluation of the staining.

## References

1. Mundy GR (1997) Mechanisms of bone metastasis. Cancer 80(8 Suppl):1546–1556
2. Green JR (2003) Antitumor effects of bisphosphonates. Cancer 97(3 Suppl):840–847
3. Coxon FP, Helfrich MH, Van't Hof R et al (2000) Protein geranylgeranylation is required for osteoclast formation, function, and survival: inhibition by bisphosphonates and GGTI-298. J Bone Miner Res 15(8):1467–1476
4. Dunford JE, Thompson K, Coxon FP et al (2001) Structure–activity relationships for inhibition of farnesyl diphosphate synthase in vitro and inhibition of bone resorption in vivo by nitrogen-containing bisphosphonates. J Pharmacol Exp Ther 296(2):235–242
5. Roelofs AJ, Thompson K, Ebetino FH et al (2010) Bisphosphonates: molecular mechanisms of action and effects on bone cells, monocytes and macrophages. Curr Pharm Des 16(27):2950–2960
6. van Beek E, Pieterman E, Cohen L et al (1999) Farnesyl pyrophosphate synthase is the molecular target of nitrogen-containing bisphosphonates. Biochem Biophys Res Commun 264(1):108–111
7. Fromigue O, Lagneaux L, Body JJ (2000) Bisphosphonates induce breast cancer cell death in vitro. J Bone Miner Res 15(11):2211–2221
8. Sasaki A, Boyce BF, Story B et al (1995) Bisphosphonate risedronate reduces metastatic human breast cancer burden in bone in nude mice. Cancer Res 55(16):3551–3557
9. van der Pluijm G, Que I, Sijmons B et al (2005) Interference with the microenvironmental support impairs the de novo formation of bone metastases in vivo. Cancer Res 65(17):7682–7690
10. Yoneda T, Michigami T, Yi B et al (2000) Actions of bisphosphonate on bone metastasis in animal models of breast carcinoma. Cancer 88(12 Suppl):2979–2988
11. Croucher PI, De Hendrik R, Perry MJ et al (2003) Zoledronic acid treatment of 5T2MM-bearing mice inhibits the development of myeloma bone disease: evidence for decreased osteolysis, tumor burden and angiogenesis, and increased survival. J Bone Miner Res 18(3):482–492
12. Daubine F, Le Gall C, Gasser J et al (2007) Antitumor effects of clinical dosing regimens of bisphosphonates in experimental breast cancer bone metastasis. J Natl Cancer Inst 99(4):322–330
13. Hiraga T, Williams PJ, Ueda A et al (2004) Zoledronic acid inhibits visceral metastases in the 4T1/luc mouse breast cancer model. Clin Cancer Res 10(13):4559–4567
14. Corey E, Brown LG, Quinn JE et al (2003) Zoledronic acid exhibits inhibitory effects on osteoblastic and osteolytic metastases of prostate cancer. Clin Cancer Res 9(1):295–306
15. Phadke PA, Mercer RR, Harms JF et al (2006) Kinetics of metastatic breast cancer cell trafficking in bone. Clin Cancer Res 12(5):1431–1440
16. Ottewell PD, Monkkonen H, Jones M et al (2008) Antitumor effects of doxorubicin followed by zoledronic acid in a mouse model of breast cancer. J Natl Cancer Inst 100(16):1167–1178
17. Chantry AD, Heath D, Mulivor AW et al (2010) Inhibiting activin-A signaling stimulates bone formation and prevents cancer-induced bone destruction in vivo. J Bone Miner Res 25(12):2633–2646

18. Deleu S, Lemaire M, Arts J et al (2009) Bortezomib alone or in combination with the histone deacetylase inhibitor JNJ-26481585: effect on myeloma bone disease in the 5T2MM murine model of myeloma. Cancer Res 69(13):5307–5311
19. Heath DJ, Chantry AD, Buckle CH et al (2009) Inhibiting Dickkopf-1 (Dkk1) removes suppression of bone formation and prevents the development of osteolytic bone disease in multiple myeloma. J Bone Miner Res 24(3):425–436
20. Mohanty ST, Kottam L, Gambardella A et al (2010) Alterations in the self-renewal and differentiation ability of bone marrow mesenchymal stem cells in a mouse model of rheumatoid arthritis. Arthritis Res Ther 12(4):R149
21. Trebec DP, Chandra D, Gramoun A et al (2007) Increased expression of activating factors in large osteoclasts could explain their excessive activity in osteolytic diseases. J Cell Biochem 101(1):205–220
22. Clohisy DR, Palkert D, Ramnaraine ML et al (1996) Human breast cancer induces osteoclast activation and increases the number of osteoclasts at sites of tumor osteolysis. J Orthop Res 14(3):396–402
23. Clohisy DR, Ogilvie CM, Carpenter RJ et al (1996) Localized, tumor-associated osteolysis involves the recruitment and activation of osteoclasts. J Orthop Res 14(1):2–6
24. Dhurjati R, Krishnan V, Shuman LA et al (2008) Metastatic breast cancer cells colonize and degrade three-dimensional osteoblastic tissue in vitro. Clin Exp Metastasis 25(7):741–752
25. Bodenstine TM, Beck BH, Cao X et al (2011) Pre-osteoblastic MC3T3-E1 cells promote breast cancer growth in bone in a murine xenograft model. Chin J Cancer 30(3):189–196
26. Huang Z, Cheng SL, Slatopolsky E (2001) Sustained activation of the extracellular signal-regulated kinase pathway is required for extracellular calcium stimulation of human osteoblast proliferation. J Biol Chem 276(24):21351–21358
27. Shiozawa Y, Pedersen EA, Havens AM et al (2011) Human prostate cancer metastases target the hematopoietic stem cell niche to establish footholds in mouse bone marrow. J Clin Invest 121(4):1298–1312
28. Vukmirovic-Popovic S, Colterjohn N, Lhotak S et al (2002) Morphological, histomorphometric, and microstructural alterations in human bone metastasis from breast carcinoma. Bone 31(4):529–535
29. Armstrong AP, Miller RE, Jones JC et al (2008) RANKL acts directly on RANK-expressing prostate tumor cells and mediates migration and expression of tumor metastasis genes. Prostate 68(1):92–104
30. Mendoza-Villanueva D, Zeef L, Shore P (2011) Metastatic breast cancer cells inhibit osteoblast differentiation through the Runx2/CBFbeta-dependent expression of the Wnt antagonist, sclerostin. Breast Cancer Res 13(5):R106
31. Kinder M, Chislock E, Bussard KM et al (2008) Metastatic breast cancer induces an osteoblast inflammatory response. Exp Cell Res 314(1):173–183
32. Coleman RE, Marshall H, Cameron D et al (2011) Breast-cancer adjuvant therapy with zoledronic acid. N Engl J Med 365(15):1396–1405